

**The Creation of True Two-Degree-
of-Freedom Epicyclic Gear Trains**

by

Lung-Wen Tsai and Chen-Chou Lin

The Creation of True Two-Degree-of-Freedom Epicyclic Gear Trains

Lung-Wen Tsai, Associate Professor
and
Chen-Chou Lin, Graduate Research Assistant

Department of Mechanical Engineering

and

Systems Research Center

University of Maryland
College Park, MD 20742

ABSTRACT

To date, most of the multi-DOF (degree-of-freedom) epicyclic gear trains have been used as a series of one-DOF devices. Comparatively little is known with regard to the existence and synthesis of true multi-DOF epicyclic gear trains. This paper presents a systematic methodology for the identification and enumeration of the kinematic structure of true multi-DOF epicyclic gear trains. It has been shown that there exist no true two-DOF epicyclic gear trains with five or less links and, that there exist two nonisomorphic rotation graphs of six vertices and twenty nonisomorphic rotation graphs of seven vertices. An atlas of nonisomorphic displacement graphs which can be used to construct true two-DOF epicyclic gear trains with six and seven links has been developed. It is hoped that this atlas will lead to more optimum and efficient designs of machines with multiple actuating requirements such as robotic wrists, grippers and walking machines.

1. Introduction

Traditionally, mechanical systems are made-up of closed loop configurations which rely on a single input to drive the system. These, so-called, one-DOF (degree-of-freedom) mechanisms are characterized by the fact that the configuration of the system depends on one input parameter. For each given input, the output is uniquely determined regardless of the complexity of the system. One-DOF mechanisms are by far the most common type of mechanisms, and can be found in almost every kind of machines and mechanical devices. The topological synthesis of such devices have been studied extensively [2-5, 7-9, 11-14, 21].

Another group of importance is the multi-DOF systems. The characteristics of multi-DOF systems is that the configuration of the system depends on more than one input parameter. That means these mechanisms require multiple inputs in order to derive a unique output. On the other hand, with a single input, the outputs are indeterminate. The behavior of such multi-output devices will depend on the nature of the resistance opposing the motion at each of the output shafts. Multi-DOF mechanisms can be found in adders and gear differentials for adding or subtracting motion or for torque distribution. Recently, they can also be found in robotic devices such as robotic wrists, grippers and walking machines [1, 6, 15, 17].

Although mechanical systems with multiple inputs or multiple outputs have existed for many years, generally, they have been used as a series of one-DOF devices rather than as true multi-DOF mechanisms. For example, the automotive bevel-gear differential, a two-DOF mechanism with one input and two outputs, is made-up of a one-DOF gear train in series with its gear box. The second

degree of freedom is simply obtained by allowing the gear train as a unit to rotate with respect to the gear box. We have found most of the two-DOF mechanisms enumerated in [6] and [11] belong to this type of mechanisms.

With the ever increasing use of modern control theory and the demands for industrial automation and flexible manufacturing, true multi-DOF mechanisms are coming into wider use, and being used in fundamentally different ways. However, the availability of such mechanisms is relatively few. Comparatively little is known with regard to the synthesis of such mechanisms.

In what follows, we shall introduce a method for the identification of true multi-DOF epicyclic gear trains and describe a systematic methodology for the enumeration of the topological structure of these mechanisms.

2. The Topological Structure of Epicyclic Gear Trains

(a) **Structural Characteristics.** We shall limit our investigation to those mechanisms which obey the general degree-of-freedom equation. As shown previously [2, 3, 8, 16], we shall use planar graph to represent the topological structure of a mechanism. In the graph representation, links are denoted by vertices, joints by edges, and the edge connection of vertices corresponds to the joint connection of links. In order to distinguish different types of joints, the edges can be colored and/or labeled. For epicyclic gear trains, turning pairs are represented by thin edges, gear pairs by heavy edges, and the thin edges are labeled according to their axis locations in space. A labeled graph of an epicyclic gear train is sometimes referred to as the displacement graph.

We shall consider only those mechanisms which obey the basic assumptions

and the fundamental rules established in the earlier papers [2, 3, 8, 16]. According to the fundamental rules [8], we can list the relationships among the number of thin edges, heavy edges, and vertices of two-DOF epicyclic gear trains as shown in Table 1.

TABLE 1. Number of Vertices vs. Number of Edges.

n	t	g
4	3	1
5	4	2
6	5	3
7	6	4
8	7	5

In Table 1, n denotes the number of vertices, t the number of thin edges, and g the number of heavy edges.

In order to automate the process of mechanism creation, vertex-vertex adjacency matrix will be used to denote the graph of a mechanism. The adjacency matrix is a symmetric matrix of order n . All the diagonal elements of the matrix are set to zero and the off diagonal elements are set to 1, or g , or 0 according to whether vertex i is connected to vertex j by a turning pair, or a gear pair, or not. For a labeled graph, the thin edges can be denoted by different symbols such as a , b , c , etc. to indicate their axis locations.

A rotation graph is defined as the graph obtained from the graph of an epicyclic gear train by deleting all the thin edges and, then, reconnect the end vertices of the heavy edges directly to their corresponding transfer vertices with thin edges. See [8] for the definition of transfer vertex. Note that,

using this definition, the number of thin edges in a rotation graph can exceed that of a conventional graph. This definition is essentially taken from Ravisankar and Mruthyunjaya [13] and is different from that defined by Freudenstein [8].

(b) **Pseudoisomorphic Graphs.** According to the fundamental rules [3], the subgraph G formed by deleting all the heavy edges from the graph of an epicyclic gear train is a tree. Furthermore, if the subgraph G contains k vertices connected by thin edges of a common label, these vertices and their incident edges of the same label form a subtree H . From the mechanism point of view, vertices connected together by thin edges having a common label implies that the corresponding links in the mechanism are connected by revolute joints that share a common joint axis. Thus, it is possible to rearrange the turning pairs among these coaxial links without changing functional characteristics of the mechanism [17]. Hence, any edge in the subtree H can be replaced with a new edge of the same label. The only restriction is that the resulting subgraph remains as a tree. In theory, because of the coaxial condition, additional edges of the same label can be added to the subtree H without affecting the function of the mechanism. However, we shall exclude graphs having those kind of redundant edges since they don't satisfy the general degree-of-freedom equation. The operation of replacing an edge in the subtree H with another edge of the same label is called vertex selection.

Two graphs satisfying the fundamental rules of epicyclic gear trains [3] are said to be pseudoisomorphic if they become isomorphic under single or repeated application of vertex selection. From the above discussion, it is clear that if the graphs of two epicyclic gear trains are pseudoisomorphic, then their functional characteristics are identical.

3. True Multi-DOF Epicyclic Gear Trains

(a) **Articulated Kinematic Chains.** According to Table 1, we observe that the most elementary graph of two-DOF epicyclic gear train is a four-link-chain having three thin edges and one heavy edge. Fig. 1(a) shows the functional schematic of such a kinematic chain and Fig. 1(b) shows its corresponding graph. As shown in Fig. 1(b), thin edges 1-4 and 3-4 share a common label, b , which implies that links 1, 3 and 4 are coaxial. Hence, the joints among these coaxial links can be rearranged according to the definition of vertex selection. Fig. 1(c) shows such a rearrangement and Fig. 1(d) shows the corresponding graph. It is obvious that Fig. 1(d) is obtained by adding edge 1-3 to and removing edge 1-4 from the graph of Fig. 1(b).

The graph shown in Fig. 1(b) is a block but the one shown in Fig. 1(d) is not, since it contains an articulation point [10]. The mechanism shown in Fig. 1(c) consists of two kinematic chains which have one common link but no common joints. More specifically, it is made up of a three-link chain (links 1, 2, and 3) in series with a two-link chain (links 3 and 4) with link 3 as the common link. A multi-DOF kinematic chain which is made-up of two or more kinematic chains with one common link but no common joints is called an articulated kinematic chain as opposed to a fully closed-loop kinematic chain. The common link corresponding to the articulation point in graph is called the cut-link since an articulated kinematic chain can be broken into two subchains by cutting the chain at the common link.

As another example, Fig. 2(a) shows the schematic of a contra-rotation gear train depicted in [2] and Fig. 2(b) shows the corresponding graph. Applying the vertex selection procedure, it can be shown that the functional

schematic shown in Fig. (2c) and its corresponding graph shown in Fig. 2(d) are pseudoisomorphic with that of Figs. 2(a) and 2(b), respectively. We note that the articulation point in Fig. 2(d) is vertex 4. In this regard, the contra-rotation gear train is composed of two kinematic chains. The first is made-up of links 1, 2, 3, and 4, and the second links 4, 5, 6 and 7. Both kinematic chains are single-DOF epicyclic gear trains. Link 4 serves as the common link to transfer motion or torque from one kinematic chain to the other.

In general, a kinematic chain is considered to be articulated, if under one or repeated application of vertex selection, one of its pseudoisomorphic graphs contains an articulation point. The link corresponding to the articulation point serves as the common link for the two subchains. Each subchain can be a simple two-link chain or a gear train having one or multiple degrees of freedom. It can be shown that a single-DOF epicyclic gear train has no cut-link; a two-DOF epicyclic gear train has at most one cut-link; and, in general, an n -DOF epicyclic gear train has at most $n-1$ cut-links.

The synthesis of articulated kinematic chains can usually be decoupled into that of several kinematic chains. It is quite straight-forward. In what follows, we shall concentrate ourselves on the synthesis of true multi-DOF epicyclic gear trains.

(b) Identification of True Two-DOF Epicyclic Gear Trains. A true multi-DOF epicyclic gear train is defined as a closed-loop kinematic chain with no cut-links. Since a labeled graph with no articulation point can sometimes be reconfigured into an articulated one, it appears that it would be necessary to apply the vertex selection procedure to a graph in as many dif-

ferent ways as possible in order to test the validity of a true multi-DOF kinematic chain. However, a graph with k vertices connected to each other with thin edges of a common edge label can have as many as $(k)^{k-2}$ pseudoisomorphic graphs. It would be difficult, if not impossible, to derive all the pseudoisomorphic graphs as the number of edges having a common edge label increases. In the following, we shall present a simple algorithm for the detection of an articulation point in a labeled graph.

As discussed previously, the graph of an articulated two-DOF epicyclic gear train can be decomposed into two components. One component must be a single-DOF epicyclic gear train while the other can be a single-DOF epicyclic gear train or a two-link chain. When these two components are transformed into rotation graphs, the articulation point becomes the one and only vertex that belongs to both rotation graphs. In the case when one component is a two-link chain, the two-link chain does not result in a rotation graph. Therefore, the link on the outer end of the two-link chain will disappear from the rotation graph. This serves as the basis for the identification algorithm to be described below.

Step 1. Store the labeled graph in a $k \times 3$ matrix $R(i,j)$, where k equals the number of gear pairs. For each row, the elements in the first two columns denote the two end-vertices of a heavy edge and the element in the third column denotes the associated transfer vertex of the gear pair.

Step 2. Check if every vertex appears as an element in the matrix R . If any vertex does not appear in the matrix R , then the graph itself or one of its pseudoisomorphic graphs contains an articulation point. No further checking is necessary.

Step 3. Pick a pair of integers, m_1 and m_2 , such that $m_1 + m_2 = k$, and $m_1 \leq m_2$. Do the following tasks:

- (i) Choose m_1 rows of elements from the matrix R to form a group, G_1 , and the remaining m_2 rows of elements to form another group, G_2 .
- (ii) Select only the distinct vertices of G_1 to form a set, S_1 , and that of G_2 to form another set, S_2 .
- (iii) If there exists one and only one element common to both sets S_1 and S_2 , then the element is an articulation point of the graph. No further checking is necessary.
- (iv) If not, repeat steps (i) to (iii) with a different combination of rows of the matrix R . The process is repeated until all the combinations are tested.

Step 4. Repeat step 3 with another pair of numbers, m_1 and m_2 , until all the combinations of m_1 and m_2 have been tested. If no articulation points are found in all the tests, then the kinematic chain is a true two-DOF epicyclic gear train.

For example, the matrix R of the gear train shown in Fig. 1 is given by $R = (1, 2, 3)$. We notice that vertex number 4 doesn't appear in the matrix. Hence, the gear train contains a cut-link.

As another example, consider the contra-rotating gear train shown in Fig. 2. The matrix R , is given by,

$$R = \begin{pmatrix} 2 & 1 & 3 \\ 4 & 2 & 3 \\ 5 & 4 & 6 \\ 7 & 5 & 6 \end{pmatrix}$$

For $m_1 = 1$ and $m_2 = 3$, we pick one row of elements from the matrix R to form the first group, G_1 , and the remaining three rows to form the second

group, G_2 . There are four combinations. One such combination is given by:

$$G_1 = (2, 1, 3),$$

and

$$G_2 = (4, 2, 3; 5, 4, 6; 7, 5, 6).$$

Hence,

$$S_1 = (2, 1, 3),$$

and

$$S_2 = (2, 3, 4, 5, 6, 7).$$

Since vertices 2 and 3 appear in both sets, no articulation point has been found for this combination. The search has been repeated for the other combinations with no success. Hence, we proceed to the next pair of numbers.

For $m_1 = 2$ and $m_2 = 2$, we pick two rows of elements from the matrix R for the first group, G_1 , and the remaining rows of elements for the second group, G_2 . There are six combinations. Because of the symmetry between G_1 and G_2 , only three are distinct. We may choose, for example,

$$G_1 = (2, 1, 3; 4, 2, 3),$$

and

$$G_2 = (5, 4, 6; 7, 5, 6).$$

Then,

$$S_1 = (1, 2, 3, 4),$$

and

$$S_2 = (4, 5, 6, 7).$$

Since, vertex number 4 is the one and only element common to both sets, S_1 and S_2 , we conclude that the mechanism contains a cut-link. Further, the

vertices shown in S_1 form one kinematic chain and that shown in S_2 form another kinematic chain, and link 4 is the common link of the two kinematic chains. The gear train can, therefore, be rearranged as shown in Fig. 2(c). Note that if we are to apply the vertex selection procedure, it would require up to $(5)^{5-2} = 125$ vertex selections in order to identify the articulation point.

4. Methods of Enumeration

Buchsbaum and Freudenstein [3] developed an atlas of unlabeled graphs for mechanisms with up to six links. The atlas was subsequently modified by Mayourian and Freudenstein [12] based on the restrictions governing the admissible graphs of kinematic chains. Such an atlas can be used as a basis for the creation of mechanisms. First, the graphs which satisfy the relationship listed in Table 1 are selected. Then, for each of the admissible unlabeled graph, we can label it in as many structurally distinct ways as possible in accordance with the fundamental rules of epicyclic gear trains. Mayourian [11] carried out this process and obtained a number of two-DOF epicyclic gear trains with up to six links. However, a careful examination of those mechanisms revealed that most of them belong to the articulated kinematic chains. The method works well for simple mechanisms. But, as the number of links increases, the process of labeling the edges becomes quite complicated.

Another possible method of enumeration is by combining two single-DOF kinematic chains. One link from each of the two single-DOF kinematic chains can be rigidly coupled together to form a two-DOF kinematic chain. Thus, an

m-link chain combined with an n-link chain results in an $m+n-1$ link chain. In fact, most of the existing two-DOF epicyclic gear trains are designed this way. However, this type of mechanisms always contains the coupling link as a cut-link.

To form a true two-DOF epicyclic gear train, one additional link is needed. The additional link is to be connected to the above kinematic chain with a turning pair on one side and a gear pair on the opposite side of the cut-link. Further, the link to be connected to the additional link with a turning pair must also serve as the gear carrier. For example, Fig. 3(a) shows the graph of a two-DOF epicyclic gear train with a cut-link. It is obvious that the graph of Fig. 3(a) is derived from the combination of two single-DOF epicyclic gears trains. Fig. 3(b) shows the graph of a true two-DOF epicyclic gear train which is obtained by adding the seventh link to the graph of Fig. 3(a). This method of enumeration seems to work well. However, it does not ensure the identification of all the true two-DOF epicyclic gear trains. It sounds logical, but it lacks the proof of completeness.

Recently, Tsai [16] developed a generic approach based on the fundamental rules of epicyclic gear trains. In his approach, the process starts with the most elementary graphs of interest, known as the generic graphs, and increase the complexity of the kinematic chain by adding one vertex at one time. The process is similar to the conventional method of gear-train design, where the designer begins with a rather simple gear train and increases the complexity by adding one gear at a time. Each time he adds a new gear, he adds not only a gear mesh to the mechanism but also a revolute joint to support the gear.

Hence, a family of mechanisms can be generated systematically. The procedure has been successfully automated by Tsai [16] for the enumeration of one-DOF epicyclic gear trains with up to six links. In what follows, we describe how to modify this methodology for the enumeration of true two-DOF epicyclic gear trains.

From Table 1, the most elementary graph of true two-DOF epicyclic gear train seems to be a four-link-chain having three thin edges and one heavy edge as shown in Fig. 1(b). However, it has been shown earlier that its pseudoisomorphic graph, Fig. 1(d), contains an articulation point. The questions remain to be answered are: Shall we use this four-link chain as the generic graph? Or, shall we find the most elementary graphs of true two-DOF epicyclic gear trains first and, then, use them as the generic graphs for the enumeration of graphs of higher complexity?

Since a kinematic chain with a cut-link can be synthesized into one without, some true two-DOF kinematic chains will be missed if we start with the most elementary graphs of true two-DOF epicyclic gear trains. Hence, we should start with the graph of four-link chain shown in Fig. 1(b) and increase the complexity by adding one vertex at a time. Using this approach, graphs with and without articulation point will be created simultaneously and all of them will include the basic four-link chain as a subgraph. We may summarize the systematic procedure as follows:

Step 1. We start with the generic graphs of n -link chains to enumerate the graphs of $(n+1)$ -link chains. The generic graphs of n -link chains are defined as a set of conventional unlabeled graphs which are rotationally non-isomorphic to one another. A generic graph may have many different ways of

labeling its edges. All of them will be stored in vertex-vertex adjacency matrices for later manipulation.

Step 2. For each generic graph, enumerate all the unlabeled graphs of $n+1$ vertices. This is accomplished by connecting an additional vertex to one of the existing vertex with a thin edge and to any one of the remaining vertices with a heavy edge. There are $n(n-1)$ potential combinations.

Step 3. Restore the edge labels of the generic portion of each new graph enumerated in step 2 in as many different ways as the generic graph has.

Step 4. Determine the transfer vertex for each new graph. Since the edge labels of the generic portion are already known, it is only necessary to check for the change of label for the newly created fundamental circuit [8]. We have three possibilities:

- (a) If there is only one transfer vertex in the new fundamental circuit and the transfer vertex is adjacent to the newly added vertex, the graph is retained as an admissible graph.
- (b) If there is only one transfer vertex, but the transfer vertex is not adjacent to the new vertex, the graph is rejected. Under this condition, the added thin edge must have an edge-label common with its adjacent edge in the new fundamental circuit. The graph can always be reconfigured into one of the graphs enumerated in category (a) above. Since the graphs in category (a) have more ways of labeling their new edges, we choose to keep the graphs of (a) as the admissible graphs.
- (c) If there are multiple transfer vertices in the new fundamental circuit, the graph is rejected due to violation of the fundamental rules.

Step 5. Check for rotational isomorphism. Once the transfer vertex of each admissible graph is identified, the corresponding rotation graph is constructed and compared with previously enumerated graphs for rotational isomorphism. This can be accomplished by comparing their linkage characteristic polynomials [16]. If the graph is isomorphic with a previous one, it is discarded. If not, it is kept as a new rotation graph of $n+1$ vertices.

Step 6. Check for the existence of an articulation point. We use the algorithm described in the previous section to detect for an articulation point. If no articulation point is found, the graph is identified as a true two-DOF epicyclic gear train, otherwise it is identified as an articulated one.

Step 7. Check for displacement isomorphism. Label the newly added thin edge in as many different ways as possible and check for displacement isomorphism. Here, we only have to compare with those graphs which have the same rotation graph. We also choose to retain all the labeled graphs regardless of whether they are isomorphic or not. This allows us to discard rotational isomorphic graphs once they are identified as stated in step 5 and simplifies the bookkeeping of the edge labels.

Step 8. Repeat steps 2 to 7 until all the generic graphs of n vertices have been used.

5. The Creation of True Two-DOF Epicyclic Gear Trains

Using the above systematic procedure, all the graphs of true two-DOF epicyclic gear trains have been enumerated. The following illustrates the sequence of enumeration.

(a) **Four-Link Chain.** As stated earlier the most elementary graph for two-DOF epicyclic gears trains is the four-link chain shown in Fig. 1(b). The corresponding epicyclic gear train is shown in Fig. 1(a). It has been shown that this kinematic chain contains a cut-link.

(b) **Five-Link Chains.** Although the graph shown in Fig. 1(b) can be reconfigured into two pseudoisomorphic graphs, we shall not alter the basic structure of Fig. 1(b) and use it as the only generic graph for the purpose of enumeration. Hence, all the graphs enumerated will contain the graph of Fig. 1(b) as a subgraph.

There are $4 \times 3 = 12$ possible ways of adding a vertex to the graph of four-link chain. Figs. 4(a) and 4(b) show two such possibilities. In Figs. 4(a) and 4(b), 1 to 4 represent the vertices of the generic graph and 5 represents the added vertex.

The next step is to restore the edge labels of the generic portion for each of the graphs shown in Figs. 4(a) and 4(b), namely, let the label of edge $2-3 = a$, $3-4 = b$, and $4-1 = b$. Then, it becomes clear that the newly added fundamental circuits for the graphs of Figs. 4(a) and 4(b) are circuits $1-5-2-3-4-1$ and $1-5-3-4-1$, respectively, and the corresponding transfer vertices are both vertex 3. Since the transfer vertex in Fig. 4(a) is not adjacent to the new vertex, 5, it is rejected. However, the transfer vertex in Fig. 4(b) is adjacent to the new vertex. Hence, Fig. 4(b) is accepted as an admissible graph. We note that the $5-2$ edge in Fig. 4(a) must be labeled as "a" while the $5-3$ edge in Fig. 4(b) can be labeled as "a" or "c". Further, the graph shown in Fig. 4(a) can be reconfigured into the one shown in Fig.

4(b). This is the reason why the graph shown in Fig. 4(b) has been accepted as an admissible graph while the one shown in Fig. 4(a) is rejected.

At this point there is no need to check for graph isomorphism, since this is the first admissible graph enumerated. Applying the algorithm for checking articulation point, we found the graph shown in Fig. 4(b) contains an articulation point.

All the twelve combinations of graphs have been constructed and tested. The results are shown in Table 2, where the first and second columns of the g matrix represent the vertex numbers of a gear pair and the third represents the corresponding transfer vertex; the second and third columns of the t matrix represent the vertex numbers of a turning pair and the first represents the corresponding edge label. The articulation point in each graph is also shown in Table 2. We note that there are five nonisomorphic rotation graphs and seven nonisomorphic displacement graphs. All of them contain an articulation point. However, all the five nonisomorphic rotation graphs have been kept as the generic graphs for the enumeration of six-link chains.

(c) Six-Link Chains. Using the five nonisomorphic rotation graphs of five vertices as the generic graphs, we enumerated eighteen (18) nonisomorphic rotation graphs of six-link chains. However, only two were identified as true blocks which resulted in three nonisomorphic displacement graphs as shown in Fig. 5.

(d) Seven-Link Chains. Using the eighteen nonisomorphic rotation graphs of six vertices as the generic graphs, we enumerated twenty nonisomorphic rotation graphs which resulted in forty-five nonisomorphic displacement graphs as shown in Fig. 6. These graphs can be used to construct all the true

two-DOF epicyclic gear trains of seven links.

For the purpose of illustration, a typical epicyclic-gear-train is sketched for each of the graphs shown in Figs. 5 and 6.

Table 2. Two-DOF Five-Link Chains.

	^g Rotation Graphs	^t Edge Labels	Articulation Point
1	$\begin{pmatrix} 2 & 1 & 3 \\ 5 & 1 & 3 \end{pmatrix}$	$\begin{pmatrix} 1 & 3 & 2 \\ 2 & 4 & 1 \\ 2 & 4 & 3 \\ 1 & 5 & 3 \end{pmatrix} \quad \begin{pmatrix} 1 & 3 & 2 \\ 2 & 4 & 1 \\ 2 & 4 & 3 \\ 3 & 5 & 3 \end{pmatrix}$	1 or 3
2	$\begin{pmatrix} 2 & 1 & 3 \\ 5 & 1 & 4 \end{pmatrix}$	$\begin{pmatrix} 1 & 3 & 2 \\ 2 & 4 & 1 \\ 2 & 4 & 3 \\ 3 & 5 & 4 \end{pmatrix}$	1
3	$\begin{pmatrix} 2 & 1 & 3 \\ 5 & 3 & 1 \end{pmatrix}$	$\begin{pmatrix} 1 & 3 & 2 \\ 2 & 4 & 1 \\ 2 & 4 & 3 \\ 3 & 5 & 1 \end{pmatrix}$	1 or 3
4	$\begin{pmatrix} 2 & 1 & 3 \\ 5 & 3 & 4 \end{pmatrix}$	$\begin{pmatrix} 1 & 3 & 2 \\ 2 & 4 & 1 \\ 2 & 4 & 3 \\ 3 & 5 & 4 \end{pmatrix}$	3
5	$\begin{pmatrix} 2 & 1 & 3 \\ 5 & 4 & 3 \end{pmatrix}$	$\begin{pmatrix} 1 & 3 & 2 \\ 2 & 4 & 1 \\ 2 & 4 & 3 \\ 1 & 5 & 3 \end{pmatrix} \quad \begin{pmatrix} 1 & 3 & 2 \\ 2 & 4 & 1 \\ 2 & 4 & 3 \\ 3 & 5 & 3 \end{pmatrix}$	3

6. Summary

A systematic methodology has been developed for the identification and enumeration of true multi-DOF epicyclic gear trains. It has been shown that there are no true two-DOF epicyclic gear trains with five or less links. For six-link chains, there are two nonisomorphic rotation graphs which have been

labeled into three nonisomorphic displacement graphs. For seven-link chains, there are twenty nonisomorphic rotation graphs which have been labeled into forty-five nonisomorphic displacement graphs. A typical functional representation is sketched for each of these graphs. The creation of actual mechanisms has been left to practicing engineers. It is hoped that this atlas will eventually lead to more optimal designs of mechanical devices such as robotic wrists and walking machines.

7. Acknowledgement

The authors wish to thank the Systems Research Center of the University of Maryland for supporting this research through an NSF grant No. NSF-CDR-8500108.

8. REFERENCES

1. Anonymous, Aug. 1982, "Bevel Gears Make Robots's Wrist More Flexible," Machine Design, Vol. 54, No. 18, p. 55.
2. Buchsbaum, F., 1968, "Structural Classification and Type Synthesis of Mechanisms with Multiple Elements," Eng. ScD Dissertation, Columbia University, Publication 67-15479, University Microfilm, Inc., Ann Arbor, MI.
3. Buchsbaum, F. and Freudenstein, F., 1970, "Synthesis of Kinematic Structure of Geared Kinematic Chains and Other Mechanisms," Journal of Mechanisms, Vol. 5, pp. 357-392.
4. Crossley, F.R.E., Feb. 1965, "A Contribution to Gruebler's Theory in the Number Synthesis of Plane Mechanisms," ASME Journal of Engineering for Industry, pp. 1-5.
5. Crossley, F.R.E., 1965, "The Permutations of Kinematic Chains of Eight Members or less From the Graph-Theoretic Viewpoint," Developments in Theoretical and Applied Mechanics, Vol. 2, Pergamon Press, pp. 467-486.
6. Datseris, P., and Palm, W., 1984, "Principles of the Development of Mechanical Hands Which Can Manipulate Objects by Means of Active Control," ASME Journal of Mechanisms, Transmissions and Automation in Design, Vol. 107, No. 2, pp. 148-156.
7. Erdman, A.G., and Bowen, J., Dec. 1981, "Type and Dimensional Synthesis of Casement Window Mechanism," Mechanical Engineering, Vol. 103, pp. 46-55.

8. Freudenstein, F., Feb. 1971, "An Application of Boolean Algebra to the Motion of Epicyclic Drives," ASME Journal of Engineering for Industry, Vol. 93, Series B, pp. 176-182.
9. Freudenstein, F., and Maki, E.R., 1979, "The Creation of Mechanisms According to Kinematic Structure and Function," The International Journal of Architecture and Design, Environment, and Planning B, Vol. 6, pp. 375-391.
10. Gibbons, A., 1985, Algorithmic Graph Theory, Cambridge University Press, Cambridge, London, Great Britain.
11. Mayourian, M., 1985, "The Creation of Mechanisms According to the Separation of Kinematic Structure and Function and Its Partial Automation," Eng. ScD. Dissertation, Columbia University.
12. Mayourian, M., and Freudenstein, F., Dec. 1984, "The Development of an Atlas of the Kinematic Structures of Mechanisms," ASME Journal of Mechanisms, Transmissions, and Automation in Design, Vol. 106, pp. 458-461.
13. Ravisankar, R., and Mruthyunjaya, T.S., 1985, "Computerized Synthesis of the Structure of Geared Kinematic Chains," Mechanisms and Machine Theory, Vol. 20, No. 5, pp. 367-387.
14. Sohn, W.J., and Freudenstein, F., Sept. 1986, "An Application of Dual Graphs to the Automatic Generation of the Kinematic Structures of Mechanisms, ASME Journal of Mechanisms, Transmissions and Automation in Design, Vol. 108, No. 3, pp. 392-398.

15. Stackhouse, T., 1979, "A New Concept in Wrist Flexibility," Proceedings of the 9th International Symposium on Industrial Robots, Washington, DC, pp. 589-599.
16. Tsai, L.W., Sept. 1987, "An Application of the Linkage Characteristic Polynomial to the Topological Synthesis of Epicyclic Gear Trains," ASME Journal of Mechanisms, Transmissions, and Automation in Design, Vol. 109, No. 3, pp. 329-336.
17. Tsai, L.W., March 31 - April 3, 1987, "The Kinematics of Robotic Bevel-Gear Trains," Proceedings of the 1987 IEEE International Conference on Robotics and Automation, Raleigh, NC, pp. 1811-1817, also accepted for publication in the IEEE Journal of Robotics and Automation.
18. Uicker, J.J., and Raicu, A., 1975, "A Method for the Identification and Recognition of Equivalence of Kinematic Chains," Journal of "Mechanisms and Machine Theory, Vol. 10, pp. 375-383.
19. Yan, H.S., and Hall, A.S., July 1981, "Linkage Characteristic Polynomials: Definitions, Coefficient by Inspection," ASME Journal of Mechanisms, Transmissions, and Automation in Design, Vol. 103, No. 3, pp. 578-584.
20. Yan, H.S., and Hall, A.S., Jan. 1982, "Linkage Characteristic Polynomials: Assembly Theorem, Uniqueness," ASME Journal of Mechanisms, Transmissions, and Automation in Design, Vol. 104, No. 2, pp. 11-20.
21. Yan, H.S., and Hwang, W.M., Dec. 1983, "A Method for the Identification of Planar Linkage Chains," ASME Journal of Mechanisms, Transmission, and Automation in Design, Vol. 105, No. 4, pp. 658-662.

Captions for Figures

Fig. 1. A Four-link Chain and its Pseudoisomorphic Mechanism With a Cut-link.

Fig. 2. The Contra-rotation Gear Train.

Fig. 3. The Creation of a True Two DOF Epicyclic Gear Train.

Fig. 4. Two Different Graphs Derived From Fig. 1(b), But Only One is Admissible.

Fig. 5. Six-link Epicyclic Gear Trains.

Fig. 6. Seven-link Epicyclic Gear Trains.

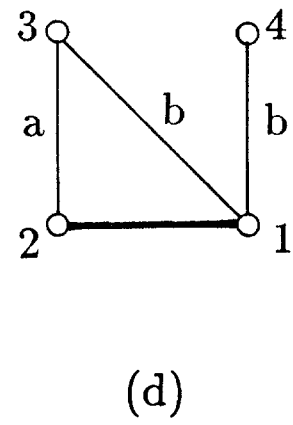
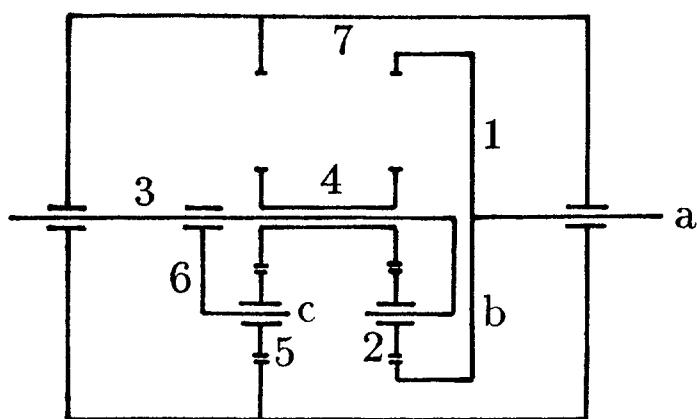
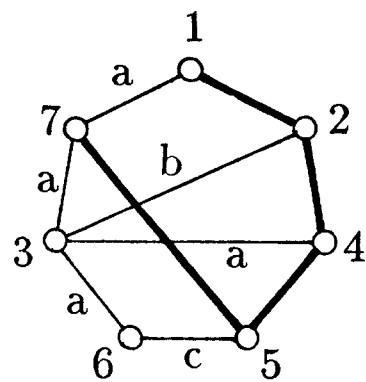


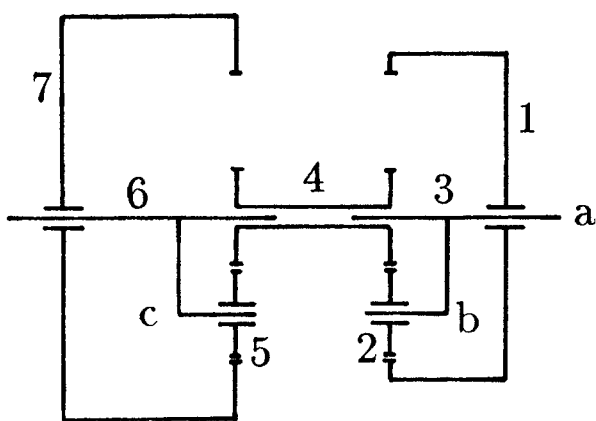
Fig. 1. A Four-Link Chain and Its Pseudoisomorphic Mechanism with a Cut-Link.



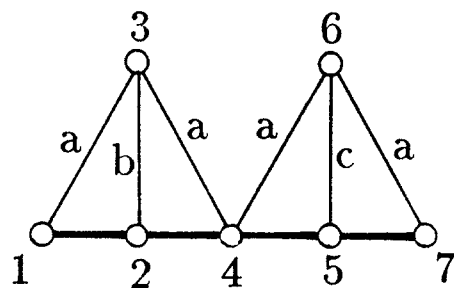
(a)



(b)



(c)



(d)

Fig. 2. The Contra-Rotation Gear Train.

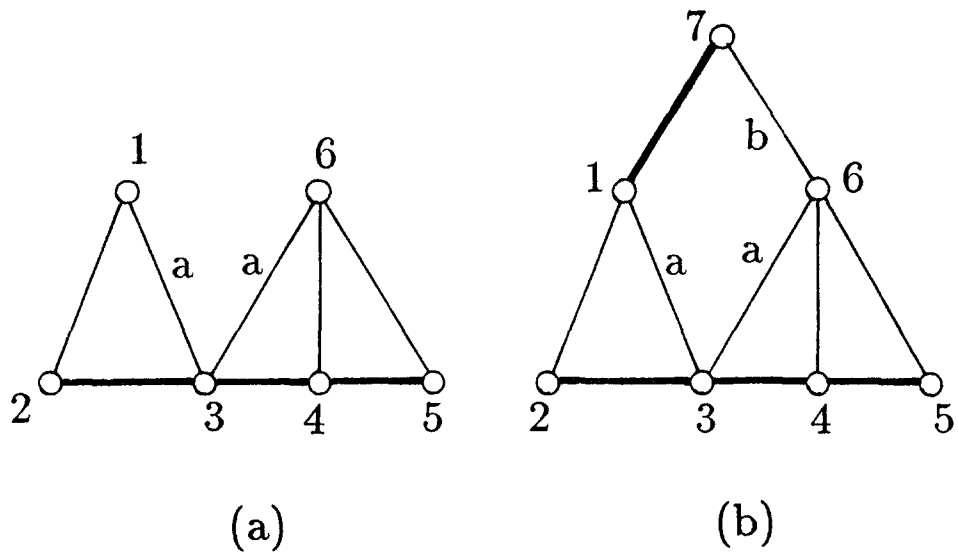
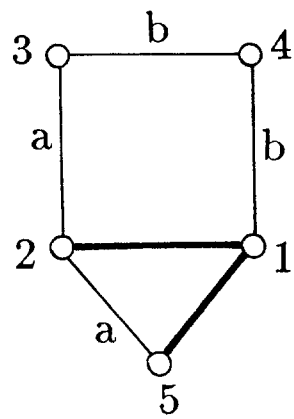
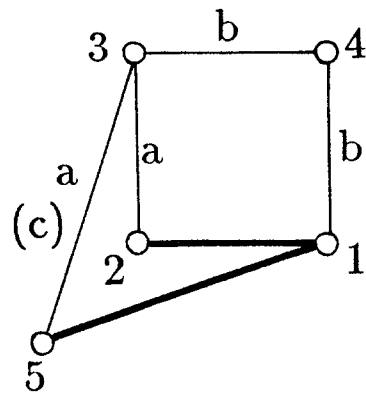


Fig. 3. The Creation of a True Two DOF Epicyclic Gear Train.

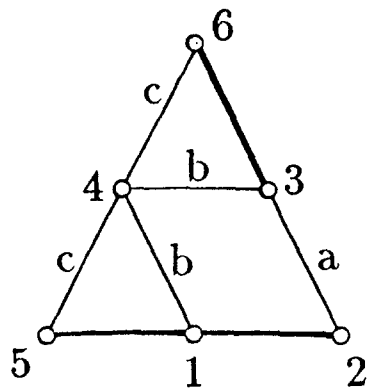


(a)

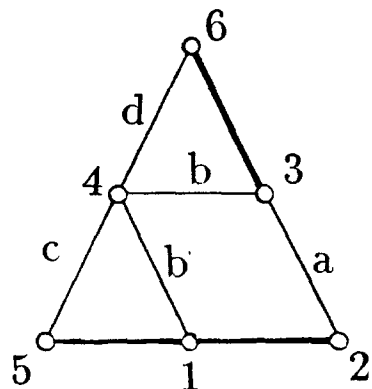
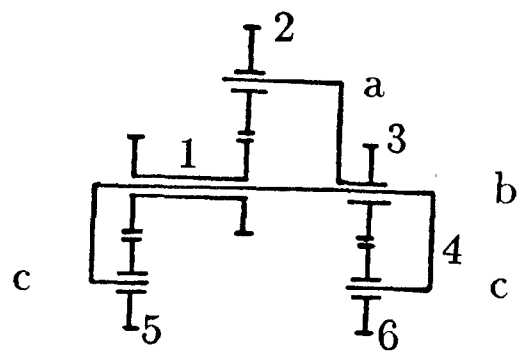


(b)

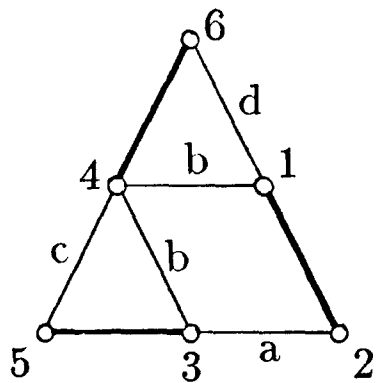
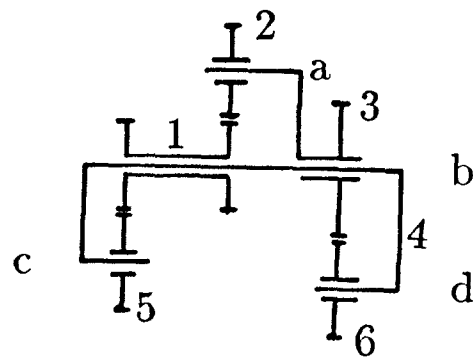
Fig. 4. Two Different Graphs Derived from Fig. 1(b),
but Only One is Admissible.



6-1-1



6-1-2



6-2-1

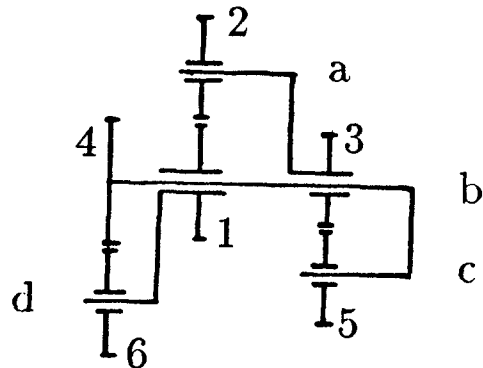
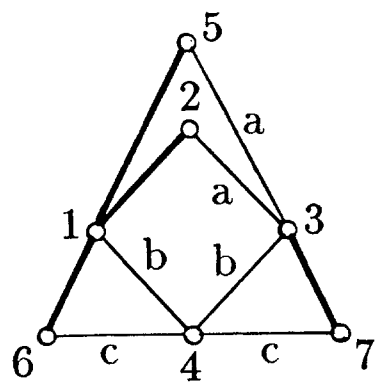
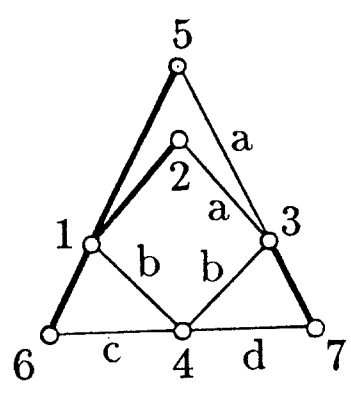
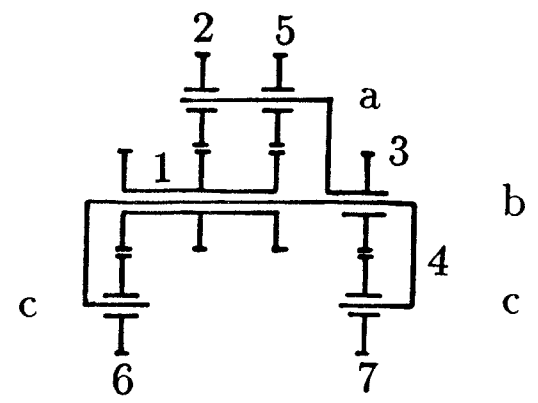


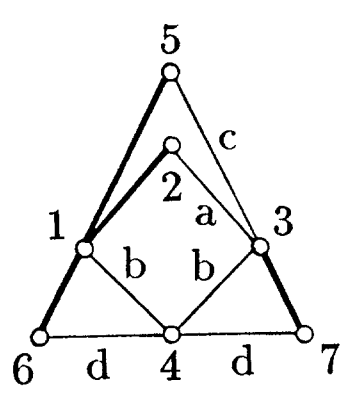
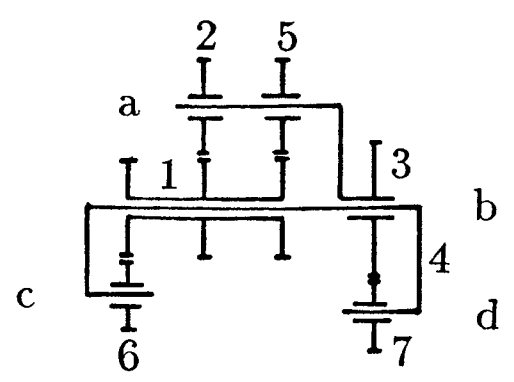
Fig. 5. Six-Link Epicyclic Gear Trains.



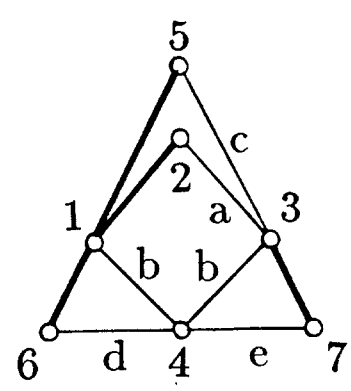
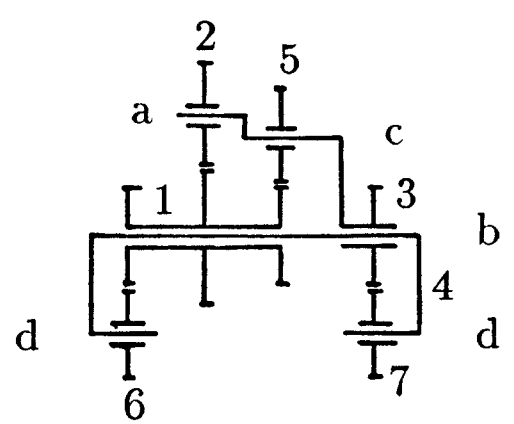
7-1-1



7-1-2



7-1-3



7-1-4

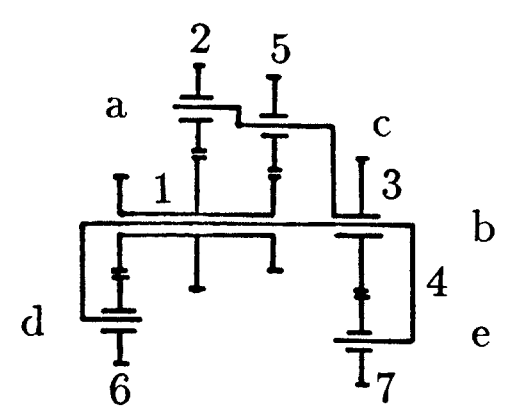
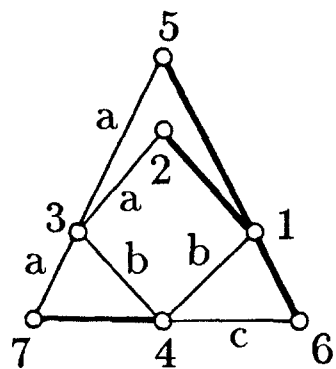
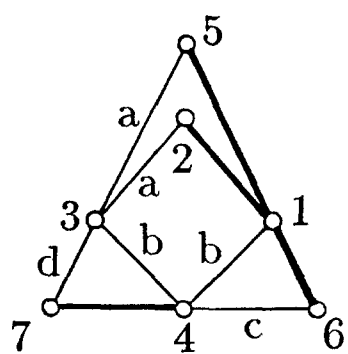
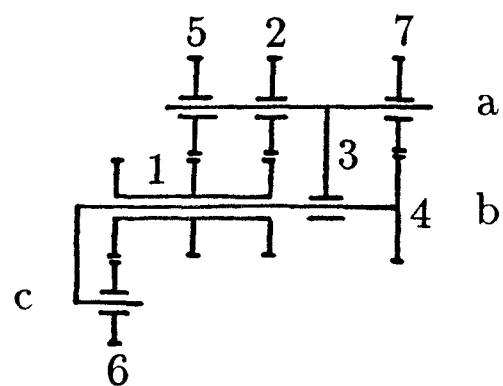


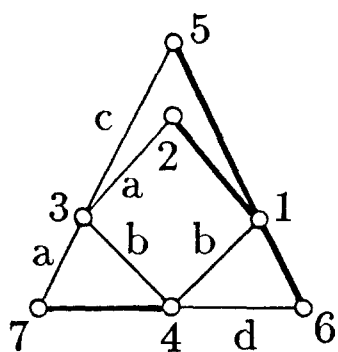
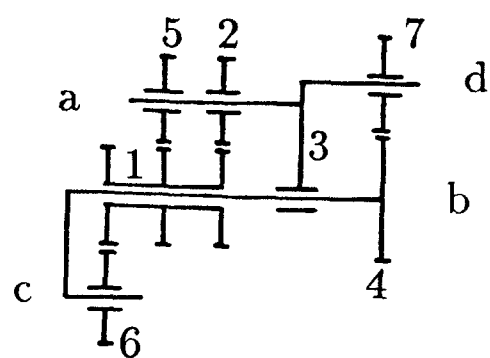
Fig. 6. Seven-Link Epicyclic Gear Trains.



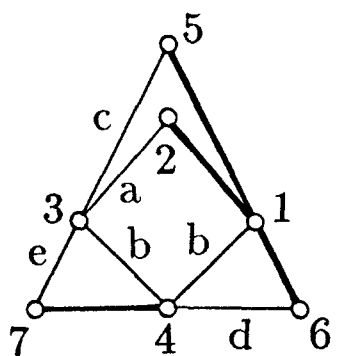
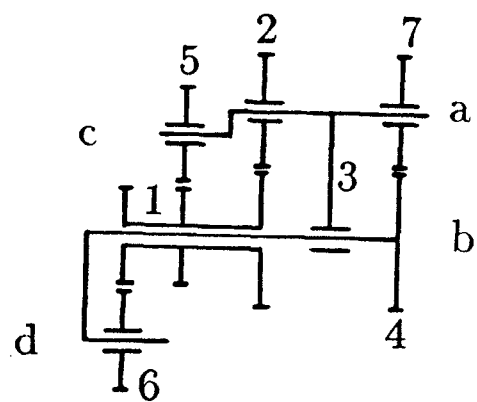
7-2-1



7-2-2



7-2-3



7-2-4

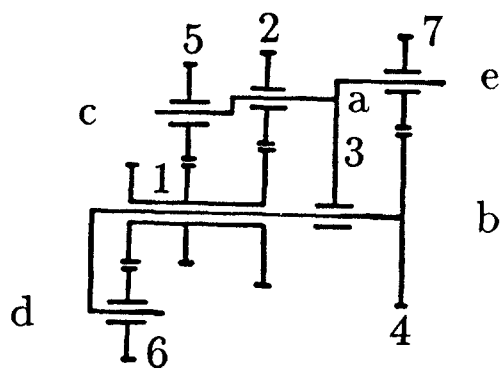
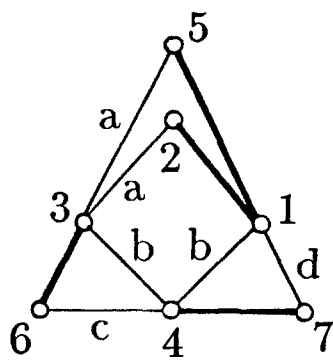
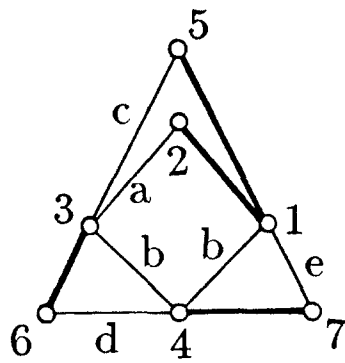
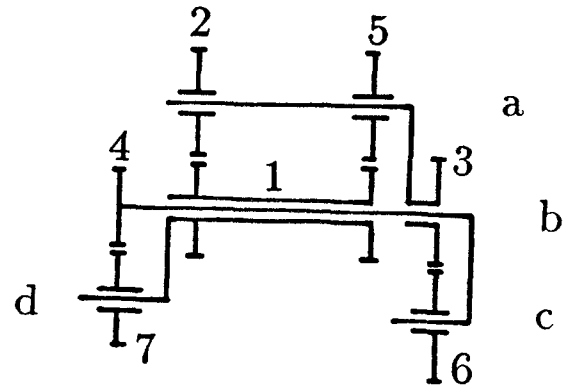


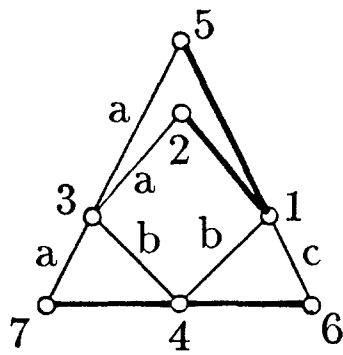
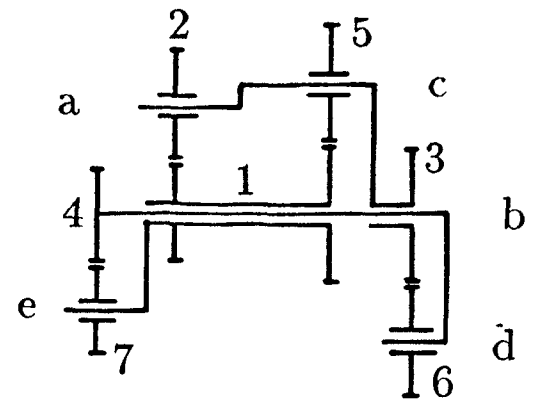
Fig. 6. (continued)



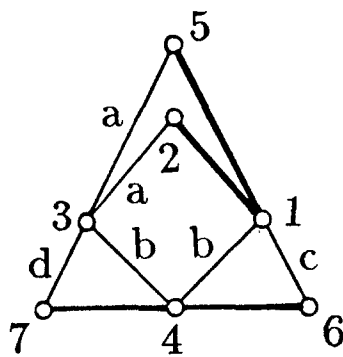
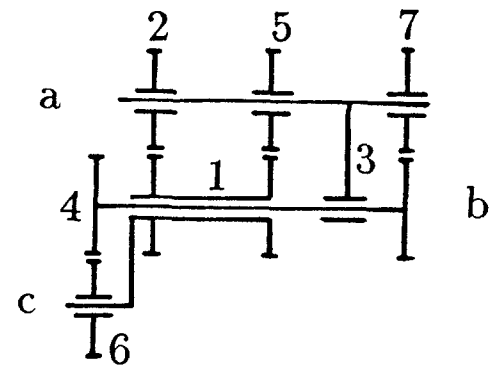
7-3-1



7-3-2



7-4-1



7-4-2

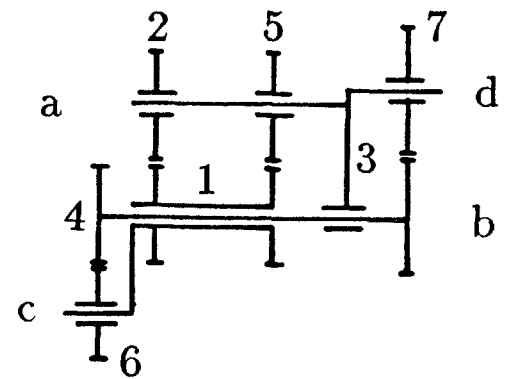
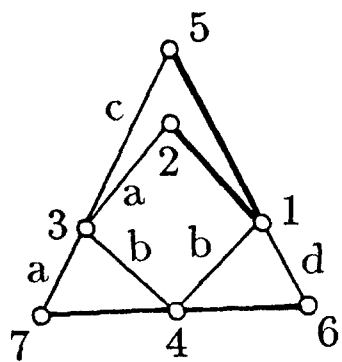
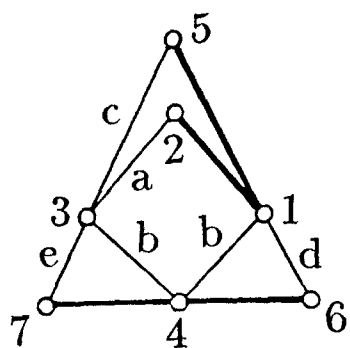
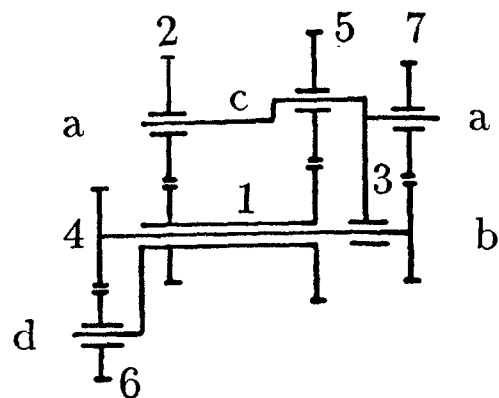


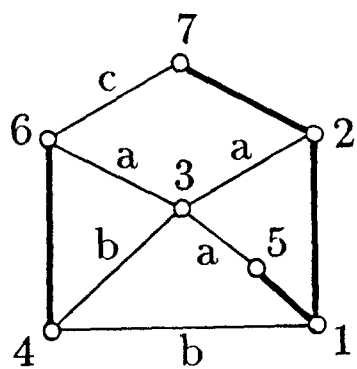
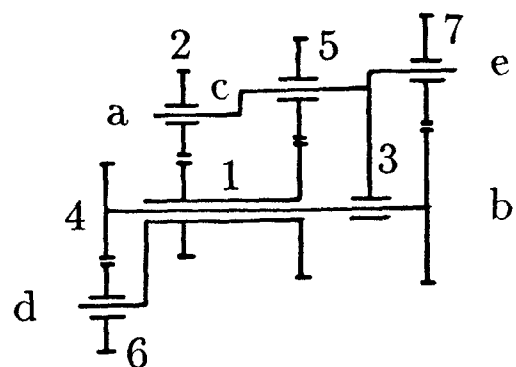
Fig. 6. (continued)



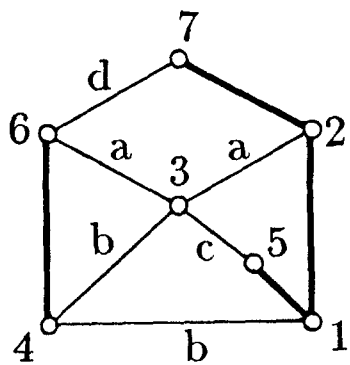
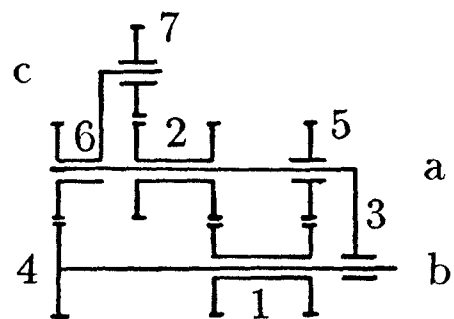
7-4-3



7-4-4



7-5-1



7-5-2

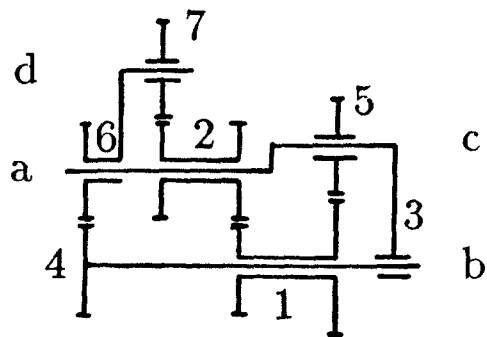
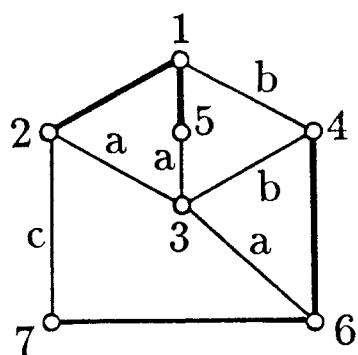
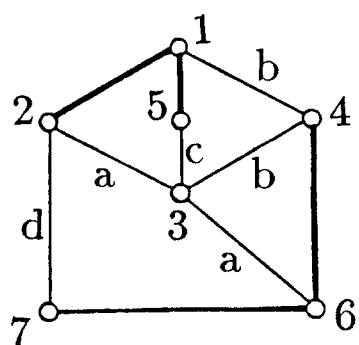
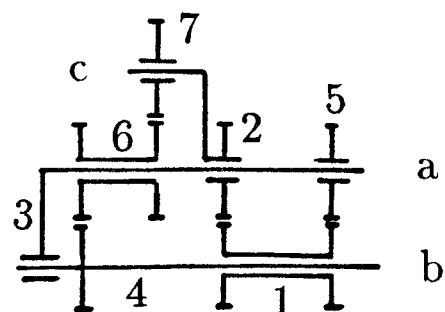


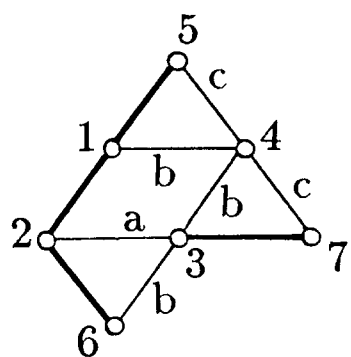
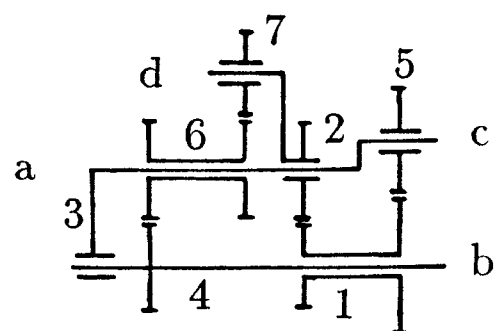
Fig. 6. (continued)



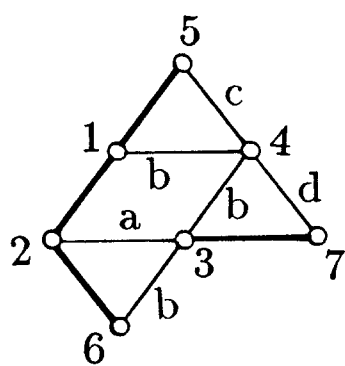
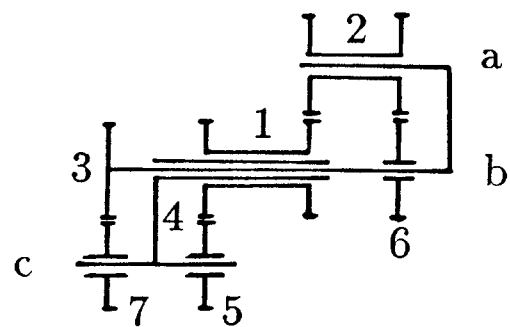
7-6-1



7-6-2



7-7-1



7-7-2

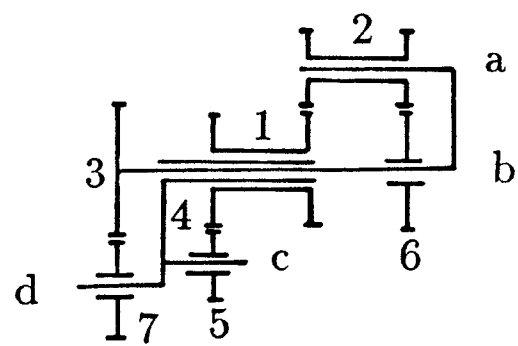
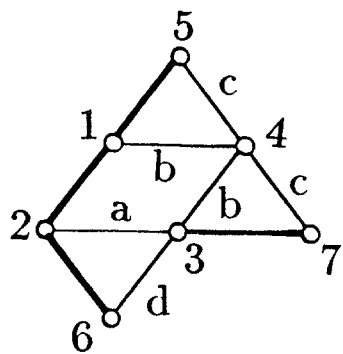
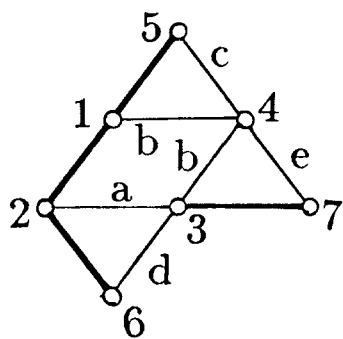
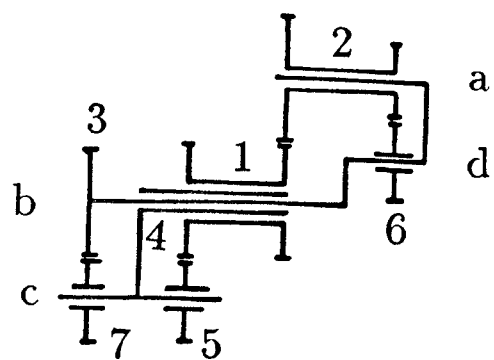


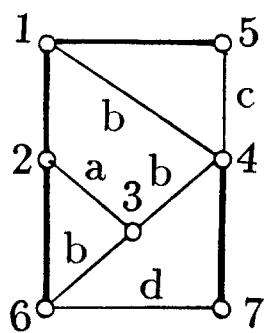
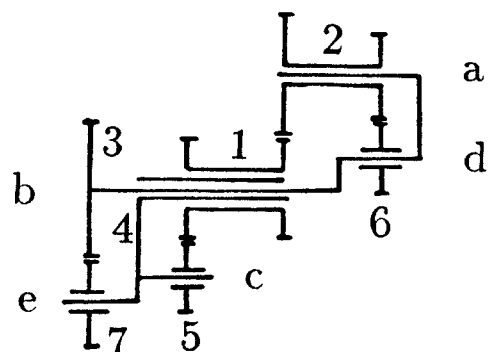
Fig. 6. (continued)



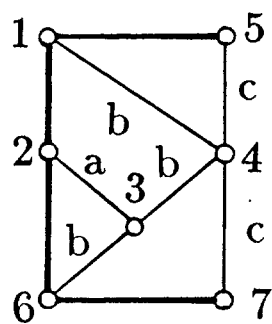
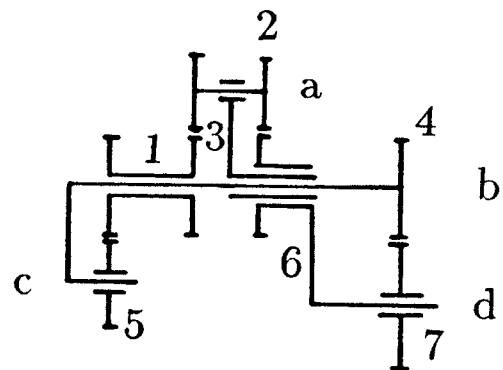
7-7-3



7-7-4



7-8-1



7-9-1

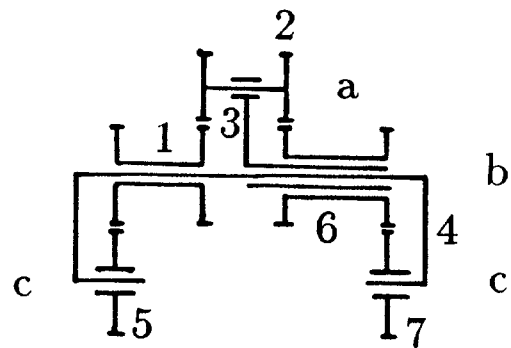
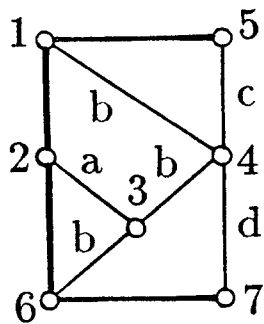
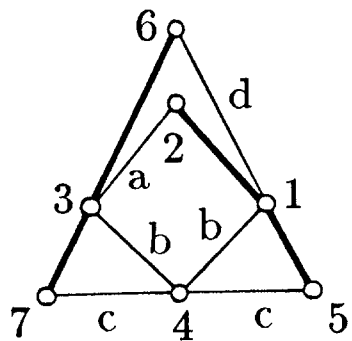
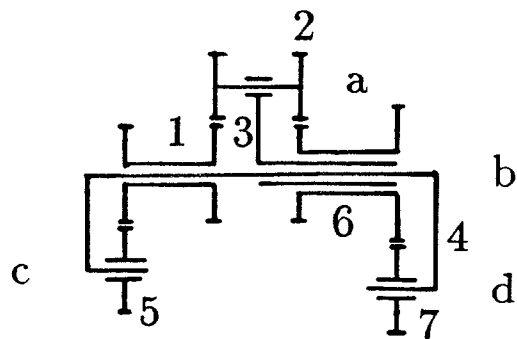


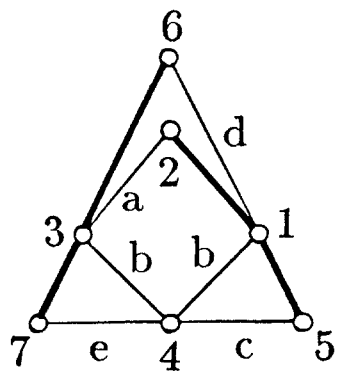
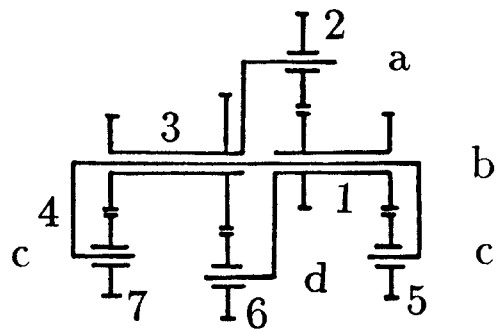
Fig. 6. (continued)



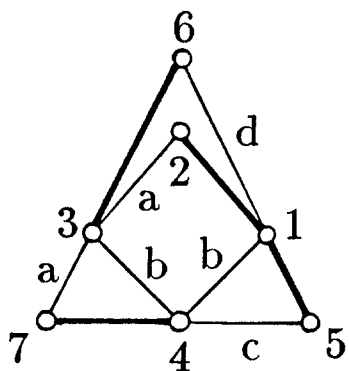
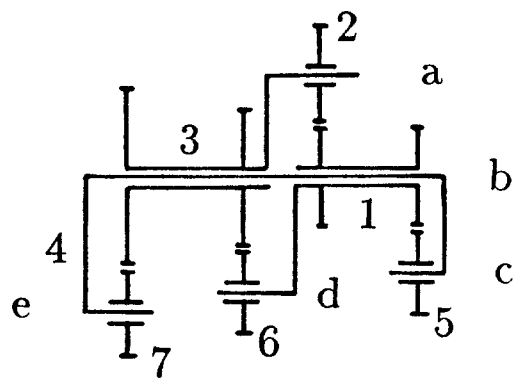
7-9-2



7-10-1



7-10-2



7-11-1

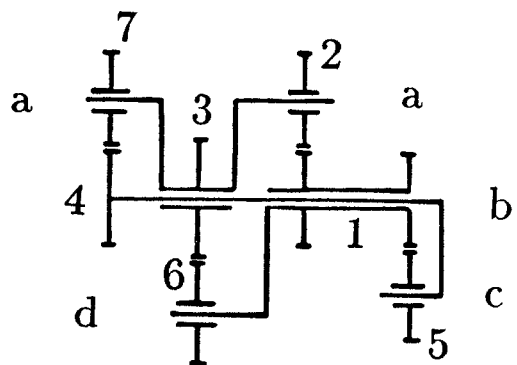
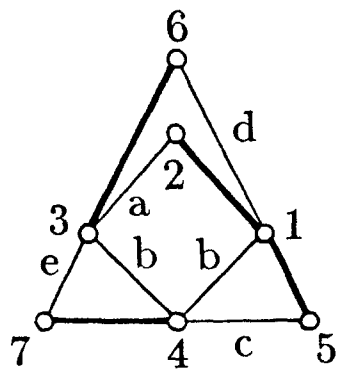
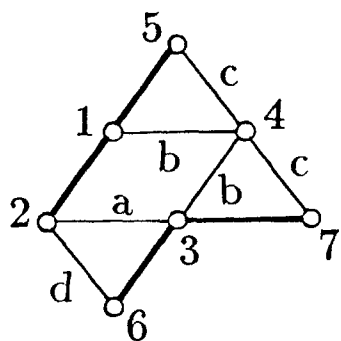
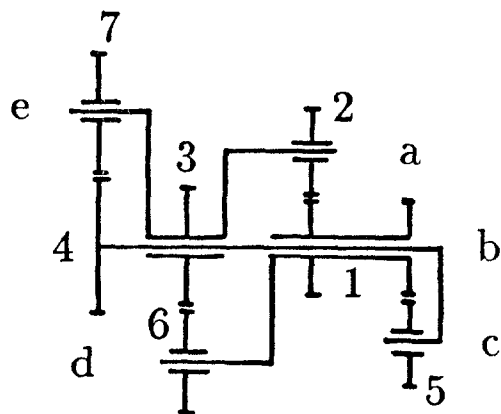


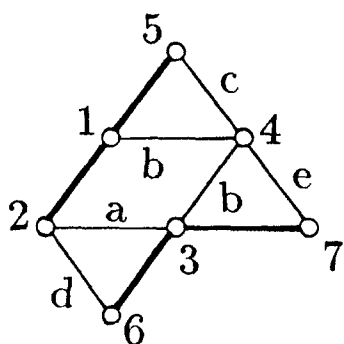
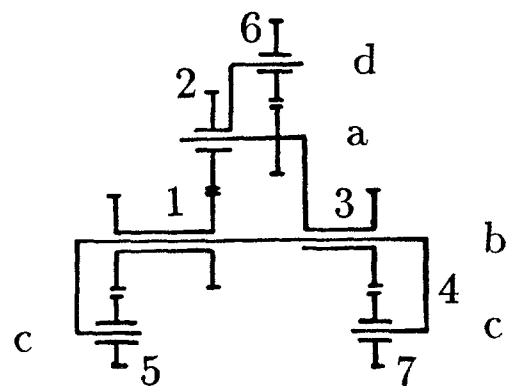
Fig. 6. (continued)



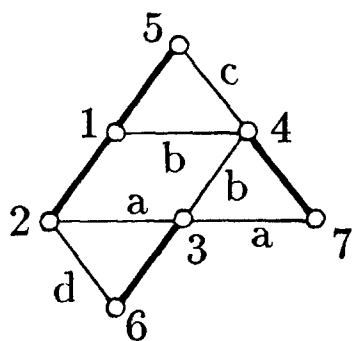
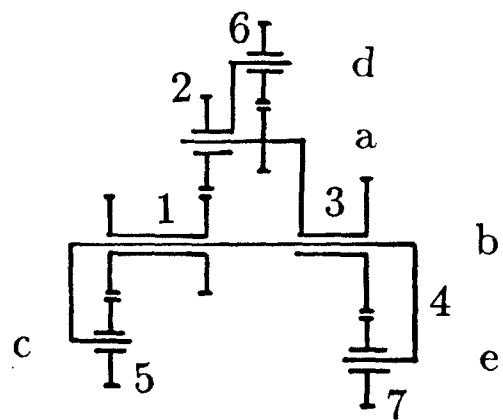
7-11-2



7-12-1



7-12-2



7-13-1

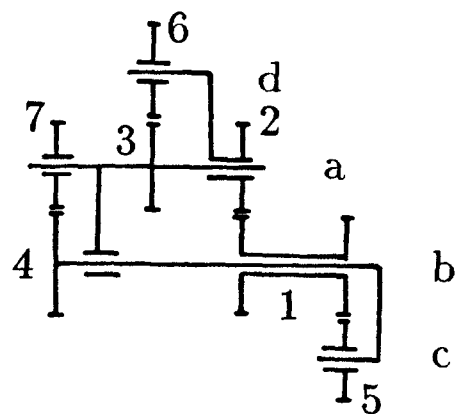
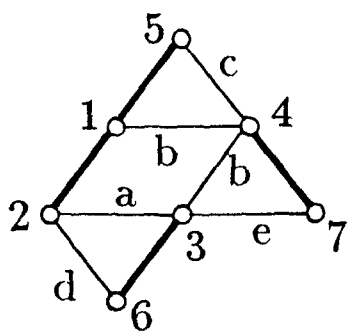
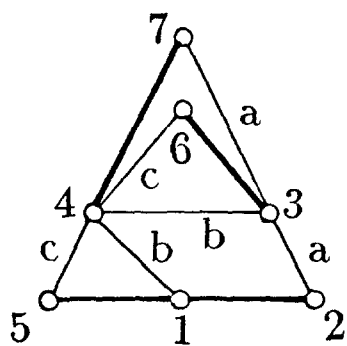
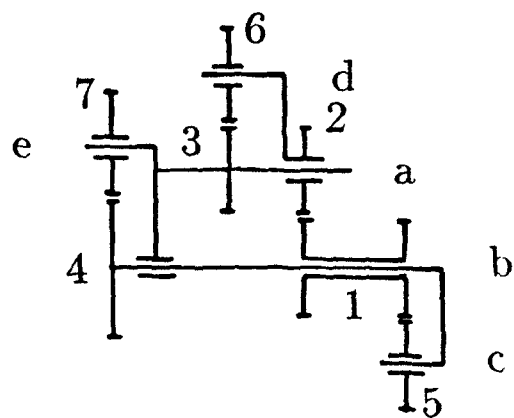


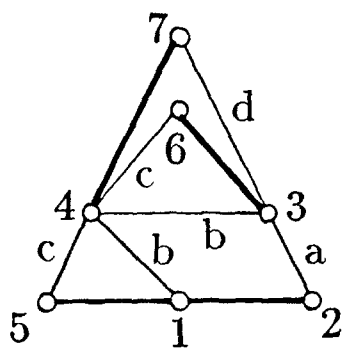
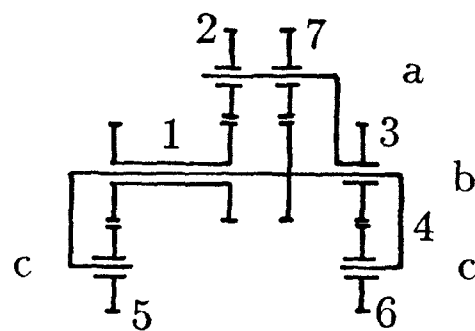
Fig. 6. (continued)



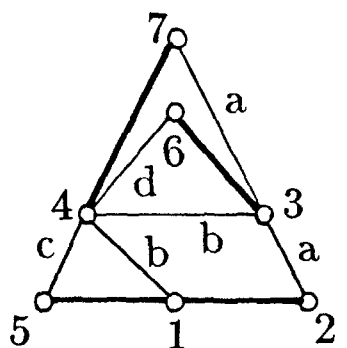
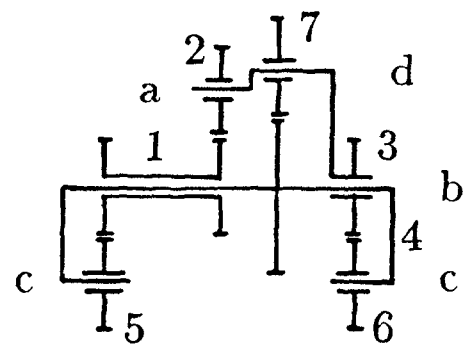
7-13-2



7-14-1



7-14-2



7-14-3

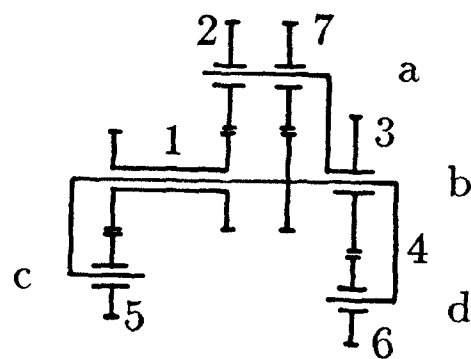
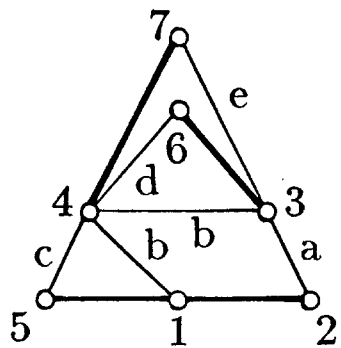
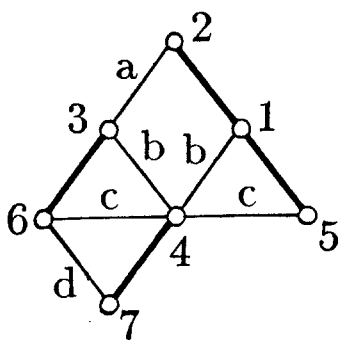
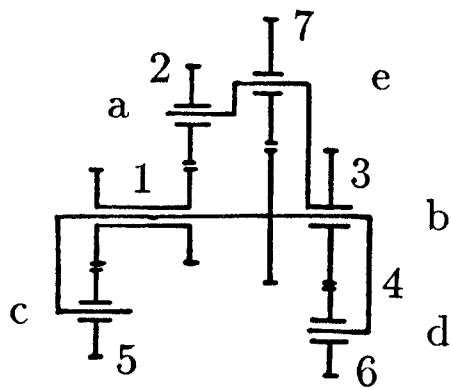


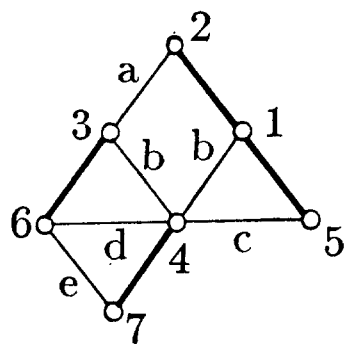
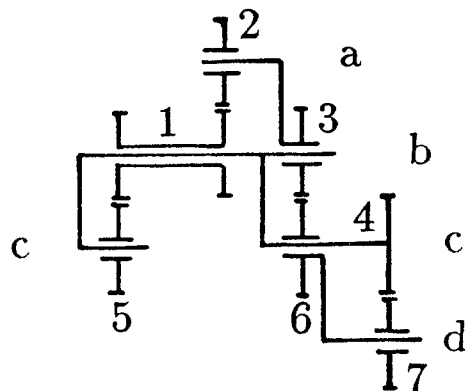
Fig. 6. (continued)



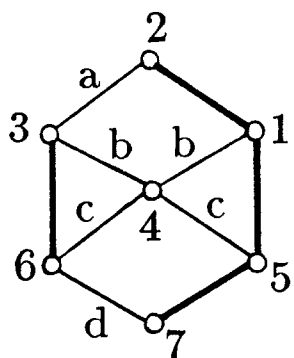
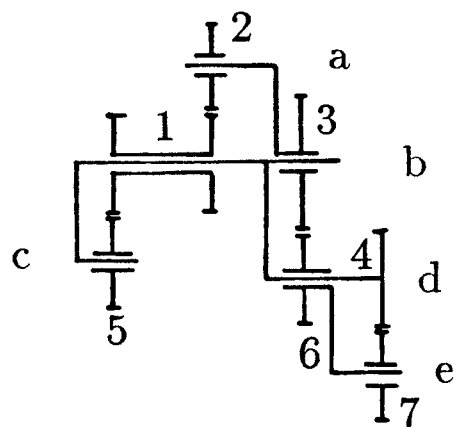
7-14-4



7-15-1



7-15-2



7-16-1

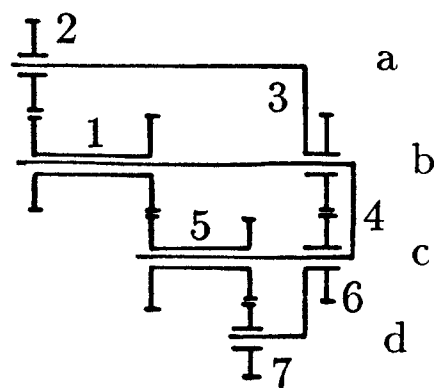
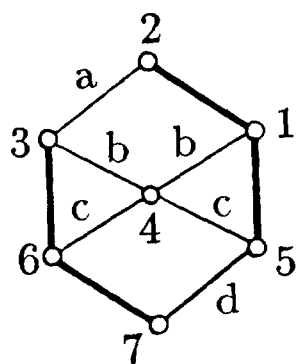
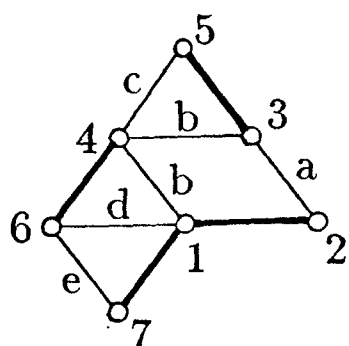
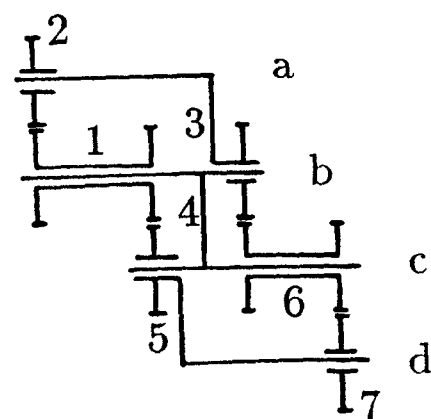


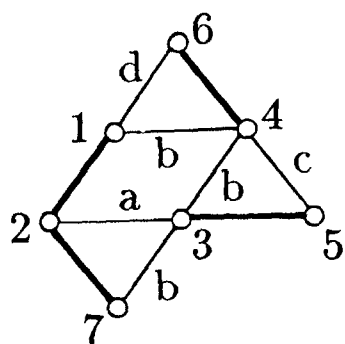
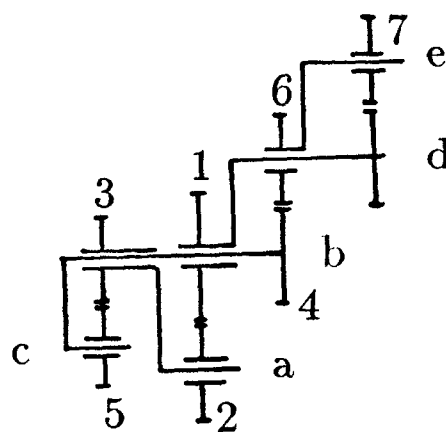
Fig. 6. (continued)



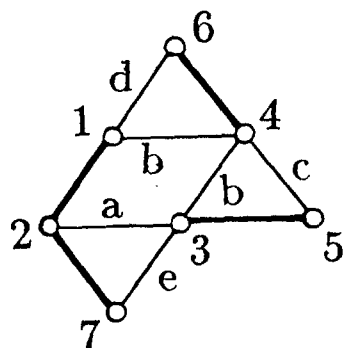
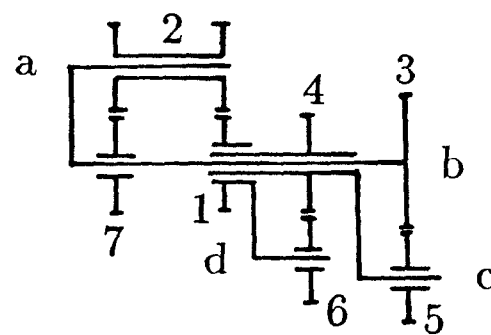
7-17-1



7-18-1



7-19-1



7-19-2

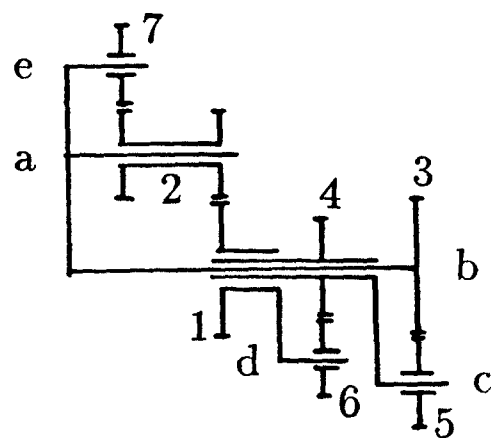
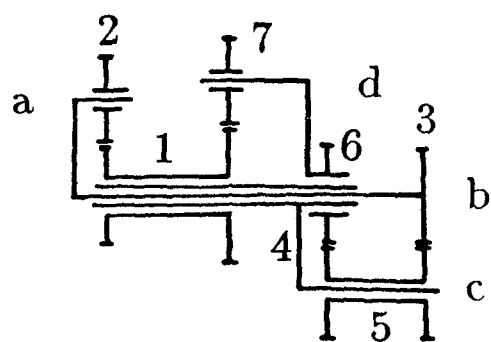
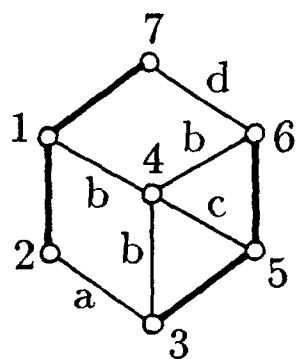


Fig. 6. (continued)



7-20-1
Fig. 6. (continued)